

UNREINFORCED MASONRY BASEMENT WALLS - A COMPARISON OF THEORETICAL DESIGN APPROACHES AND NUMERICAL SIMULATIONS

W. JÄGER¹, T. VASSILEV², J. HOFFMANN³ & P. SCHÖPS⁴

¹Prof. Dr.-Ing., ²Doz. Dr.-Ing., ³MSc, ⁴Dipl.-Ing.
Chair of Structural Design
Faculty of Architecture
Technische Universität Dresden - Germany

SUMMARY

Due to a recent accumulation of damage in newly constructed masonry basement walls, their regulations in present design codes was doubted by several researchers and practical engineers (see Ackermann 2006). In the present paper the authors try to provide an in depth insight into this topic. The first part of the paper presents and examines an experimental justification of the active earth pressure condition as suggested by the German Masonry Code (DIN 1053) and Eurocode 6 (EC 6). In the second part the focus is put on the analytical model underlying the design procedures according to DIN and EC 6, where great attention is paid to the fundamental assumptions and inherent limitations. Thereupon it is shown that for many practical situations (mainly uniaxial vertical load transfer) the analytical approach is close to reality, whereas in some cases the load bearing capacity is substantially underestimated. These conclusions are based on results from numerical analyses of high complexity and reliability. Finally, construction solutions are presented for practical cases, where design code calculations predict insufficient capabilities to withstand out of plane horizontal loads.

INTRODUCTION

The bearing capacity of basement walls and their structural design are influenced by numerous factors that complicate the analysis performed by the structural engineer. Starting with the estimation of the acting earth pressure, which not only depends on the backfill height and optionally existent service loads, but is also influenced by the backfill material, the compaction method applied and the lateral flexibility of the basement wall itself, through the calculation of superimposed loads and resulting internal forces to the particular mechanical behaviour of masonry with its multitude of different unit-mortar-combinations, the structural behaviour of each basement wall is quite unique. Fortunately, the structural engineer's task is usually alleviated by humble architectural restraints, thus allowing a structurally safe design without the need of sophisticated calculations. With sufficient mechanical background knowledge most of the designed basement walls can be verified with little effort to meet all requirements.

EARTH PRESSURE ACTING ON BASMENT WALLS

The intensity of the earth pressure acting on basement walls mainly depends on the flexibility of the basement wall itself and the methods used for placing and compacting the backfill material. If the basement wall is flexible enough, then the earth pressure decreases depending on the degree of activation of the shear strength along potential shear surfaces in the soil. The smallest earth pressure – the so called active earth pressure – is reached, if the lateral deflection of the wall is large enough to completely activate the shear strength of the soil.

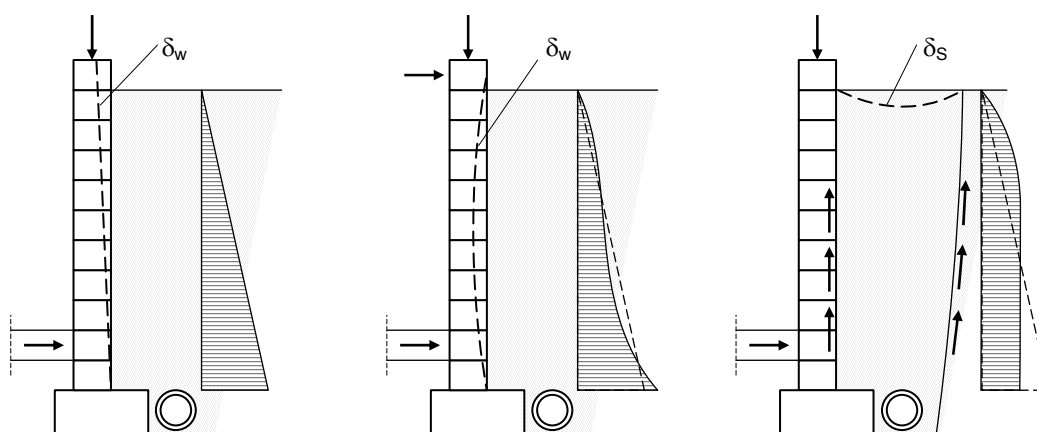


Figure 1. Effects of different lateral wall deflections and wall friction on the earth pressure distribution (δ_w = wall deflection, δ_s = settlement of the backfill material) (Broms 2007)

The wall deflection necessary to achieve this condition is mainly governed by the relative degree of soil compaction. If the backfill is systematically compacted during the construction process, the required wall movement is in the range of 0.05 to 0.1 % of the wall height; otherwise it is approx. 0.2 % of the wall height. Assuming for instance a wall height of 2.0 m and a compacted backfill, the wall has to deflect about 1–2 mm under the action of the active earth pressure to actually induce the active earth pressure condition. For uncompacted backfill material this value may increase to approx. 4 mm. However, these estimations imply a loose backfill material consisting of gravel or sand and a lateral bearing capacity of the basement wall sufficient to withstand the loading due to the compaction process. Otherwise the basement wall has to be temporarily supported or strengthened during the compaction. If glacial till with a high clay fraction (> 10–15 %) or clay is used as backfill material, the lateral deflections necessary to induce active earth pressure conditions is unequally larger, namely 1–2 % of the wall height. This problematic condition has been investigated in depth by *Tengvall* and *Broms*.

The distribution of the earth pressure along the height of the basement wall depends on the deformation of the wall, the friction between wall and backfill as well as between backfill and undisturbed soil (see Figure 1). However, the total value of the horizontal thrust is largely unaffected by the relative displacement of the wall and the location of the deflection maximum along the wall height. In contrast, the friction along the basement wall and the excavation slope affects not only the distribution of the earth pressure but also the total value of the horizontal thrust of the backfill (see Figure 1, right). If the backfill material is not artificially compacted the subsequent settlements will cause a bulging earth pressure distribution. Due to the supporting action of the friction forces the resulting earth pressure at

the bottom of the wall does not develop to its full value, whereas near the surface the earth pressure is increased by arching effects. The resulting horizontal thrust can thus be up to 20–30 % less than under ideal active conditions.

Basement walls built with common units or blocks are in most cases flexible enough to be realistically designed assuming active earth pressure conditions – as long as sand or gravel is used as backfill material. In cases where a sufficient flexibility of the basement wall is not clearly given, the structural design of the wall should be done with the assumption of the earth pressure conditions at rest.

In reaction to an accumulation of structural damage in basement walls of terraced houses in Sweden during the 1960's and 70's, an investigation into the causes was conducted by *Tengvall* (Tengvall 1968). In this study the fundamental causes for these damages were identified as the increasing distance of diaphragm walls in modern construction practice and the use of heavy machinery for the backfill compaction. Table 1 gives a brief comparison of the maximum earth pressure σ_{ho} in depth z_{cr} below the surface for several different compaction machines (with the respective layer thickness of the backfill placement and compaction).

Table 1. Earth pressure on unflexible basement walls due to compaction of a cohesive backfill material (Broms 2007)

Compaction machine	z_{cr} (m)	σ_{ho} (kN/m ²)	Layer thickness (m)
10.2 t drum roller	0.6	20	0,5
3.3 t vibration roller	0.5	19	0.5
1.4 t vibration roller	0.3	12.5	0.3
400 kg vibrating plate	0.45	16	0.4
120 kg vibrating plate	0.3	11.5	0.2

Spotka got roughly the same results (Spotka 1977). Additionally it should be noted, that depending on the local topographic, geologic and climatic conditions ground water and – in the case of high clay contents, frost heave also contribute, along with earth pressure, to the total horizontal thrust exerted onto the basement wall.

ANALYTICAL MODEL

The structural behaviour of basement walls with low imposed compressive load at the top is dominated by the earth pressure. Here the load transfer mechanism can be described as “bending with vertical compression” with emphasis on “bending”. The total value of the lateral load increases progressively with the depth of the retained soil and causes thus bending action which can only be counteracted by the vertical compression.

The design regulations of the German and European Design codes for Masonry (DIN 1053-100 resp. EC 6 part 3) concerning the necessary vertical compressive loads for uniaxially spanning basement walls are based on the work of *Mann* and *Bernhardt* (Mann&Bernhardt 1984). They rely on the following basic assumptions:

- the flexibility of the basement wall is sufficient to provide active earth pressure conditions
- due to insulation and/or waterproofing layers the friction between the backfill and the wall may be neglected; the earth pressure coefficient $K_a = 1/3$ will thus be conservative for any type of soil
- the earth pressure varies linearly with the soil depth, with the maximum value of $K_a \cdot \gamma_e \cdot h_e$ at the base of the wall (K_a earth pressure coefficient, γ_e specific weight of the backfill, h_e depth of the soil retained by the wall)

The weight of the wall γ_w should also be considered, since it considerably contributes to the bearing strength in case of low imposed loads at the top of the wall.

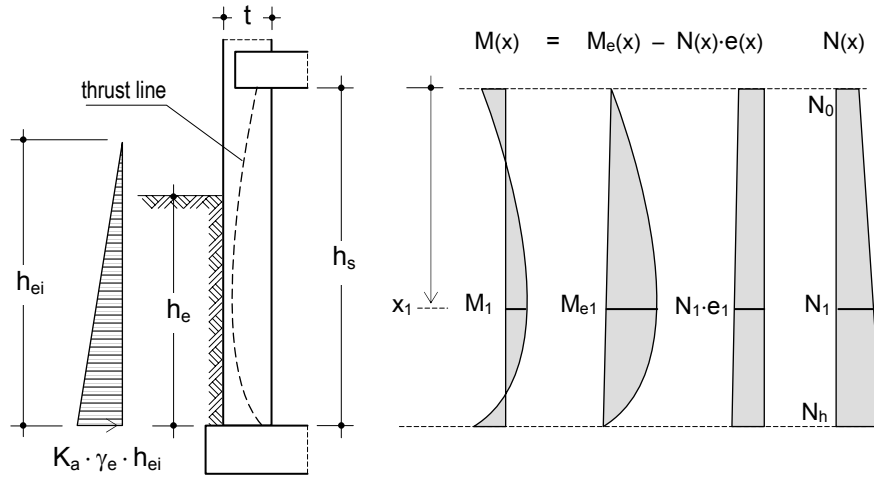


Figure 2. Loading and internal forces of uniaxially spanning basement walls with low imposed loads at the top

The increase of earth pressure due to superimposed loads on the ground surface is taken account of by means of an assumed service load q , which eventually is implied in the model in the form of a supplement (q / γ_e) to the retained soil h_e . The resulting lateral loading of the wall is presented in Figure 2 with the equivalent depth of retained soil equal to

$$h_{ei} = h_e + \frac{q}{\gamma_e} \quad (1)$$

Under the assumption of an arch-like load transfer mechanism in the vertical direction the necessary compressive load to guarantee a state of equilibrium can be determined as

$$N_1 \geq \frac{M_{el}}{2e_{lim}} \quad (2)$$

In the above expression e_{lim} is the maximally allowed eccentricity of the normal force. Since this equation holds for the location of the maximum bending moment, the necessary imposed load at the top of the wall can be calculated by including the weight of the wall

$$N_o \geq \frac{M_{el}}{2e_{lim}} - \gamma_w \cdot t \cdot x_1 \quad (3)$$

The bending moment due to the earth pressure is

$$M_{el} = \frac{K_a \cdot \gamma_e \cdot h_s^3}{6} \cdot \mu \quad (4)$$

with

$$\mu = \frac{h_{ei}^3}{h_s^3} \cdot \left(1 - \frac{h_{ei}}{h_s} + \frac{2}{3\sqrt{3}} \sqrt{\frac{h_{ei}^3}{h_s^3}} \right) \quad (5)$$

$$x_1 = h_s \sqrt{1 - \frac{h_{ei}^2}{h_s^2} \left(1 - \frac{h_{ei}}{3h_s} \right)} \quad (6)$$

Assuming that the unit weight γ_e of the backfill does not exceed the value of 20 kN/m^2 and the service load q_k on the ground surface is not greater than 5 kN/m^2 the latter expressions can be simplified to

$$\mu \approx (h_e/h_s)^2 / 2 \quad (7)$$

$$x_1 \approx h_s - h_e / 2 \quad (8)$$

If furthermore the effect of an imperfection e_a is included (an accidental eccentricity, parabolically varying along the wall height with a maximum of $0.04t$ coinciding with location of M_{el}) and the numerical values $K_a = 1/3$ and $e_{lim,k} = t/3$ are substituted, eq. (2) yields

$$N_{1,k,inf} \geq \frac{K_a \cdot \gamma_e \cdot h_s \cdot h_e^2}{12 \cdot (2e_{lim,k} - e_a)} = \frac{\gamma_e \cdot h_s \cdot h_e^2}{22,56 t} \quad (9)$$

The equations derived here are valid for use in design concepts with global safety factors. Assuming the partial factors of safety in accordance with DIN 1055-100 and EN 1990 (1.35 for permanent and 1.5 for service loads) and allowing the eccentricity to be as great as $0.45t$ in the limit state it can be shown that the solution according to eq. (9) still holds. It should be noted, that in the concept of partial safety $N_{o,k,inf}$ represents the lowest value of the imposed compressive load at the top of the wall.

The assumption of active earth pressure conditions is of course only justified, as long as the compaction of the backfill material remains moderate. However, in the process of derivation of eq. (9), several conservative assumptions have been made. The assumed earth pressure coefficient K_a , for instance, is valid for non-cohesive materials exhibiting an angle of internal friction of less than 30° . Horizontal thrusts exerted by common backfill materials can thus be up to 35 % lower. Furthermore the cohesion forces have been generally neglected and the

factor $\gamma_e = 20$ in eq. (9) is generously rounded on the safer side. Thus, even for earth pressures in the range between active pressure and pressure at rest, eq. (9) remains valid.

To this stage only the case of very low imposed compressive loads has been investigated. However, the practical design of basement walls should always include a check against a possible compressive failure as well. Here the assumption of a maximum eccentricity of $t/3$ is reasonable and thus the design check against compressive failure is simply

$$N_{o,d,sup} \leq \frac{f_d \cdot t}{3} = \frac{\eta \cdot f_k \cdot t}{3 \cdot \gamma_M} \quad (10)$$

where

f_d	the design value of the compressive strength,
t	the thickness of the wall,
η	the reduction factor covering long term effects,
f_k	the characteristic value of the compressive strength and
γ_M	the partial factor of safety for material properties.

In addition to checking the compressive load bearing capacity of the basement wall the out of plane shear strength has to be checked as well. This check commonly becomes critical, when very weak mortars are used or sealing sheeting is present at the bottom of the basement wall. Basement walls according to German construction standards usually show an ample resistance to out of plane shear forces due to earth pressure.

So far the possibility of a simultaneous load transfer in the horizontal direction (via bending action parallel to the bed joints) has been neglected. An analytical solution including these effects was presented by *Mann & Bernhardt* (Mann&Bernhardt 1984). The German Code (DIN 1053-100 2007) therefore contains a pragmatic but nonetheless appropriate rule based on this solution.

NUMERICAL COMPARISON

Due to the very limited tensile strength of masonry the load bearing behaviour under lateral loading is substantially nonlinear. Therefore numerical solution methods used to simulated masonry also have to be nonlinear in order to obtain sensible results. Among the use of nonlinear finite element codes the transfer matrix method for beam structures has been adapted by the authors to accommodate cracking and nonlinear continuous compressive behaviour particularly observed in masonry and unreinforced concrete structures. This method uses the uniaxial solution presented in the preceding part of this paper.

Transfer Matrix Method

A predecessor of the applied procedure was presented in great detail in Vassilev et al. (2004). Due to its nonlinear features the solution method is by nature iterative and constitutes an uniaxial model of the basement wall. If the wall is divided into sufficiently small sections the converged solutions can be taken as very accurate.

The following example considers a typical basement wall which exhibits an uniaxial load transfer mechanism (length \gg height) and the soil depth equals the free wall height. Here a discretisation resulting in 20 segments turned out to be sufficiently dense.

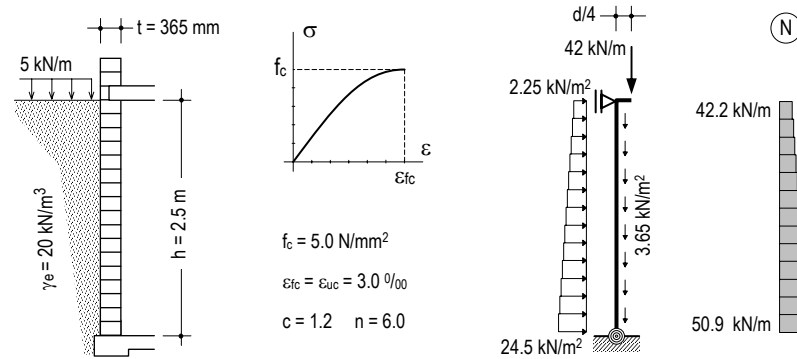


Figure 3. Example basement wall, idealised model with loading situation and assumed material behaviour under compression

Due to the prescribed eccentricity at the top of the wall (caused by the deformation of the concrete slab supported by the basement wall) the displaced shape during the construction stage (without earth pressure) is opposite to the final one under earth pressure exposure. The maximal displacement amounts to 0.16 mm.

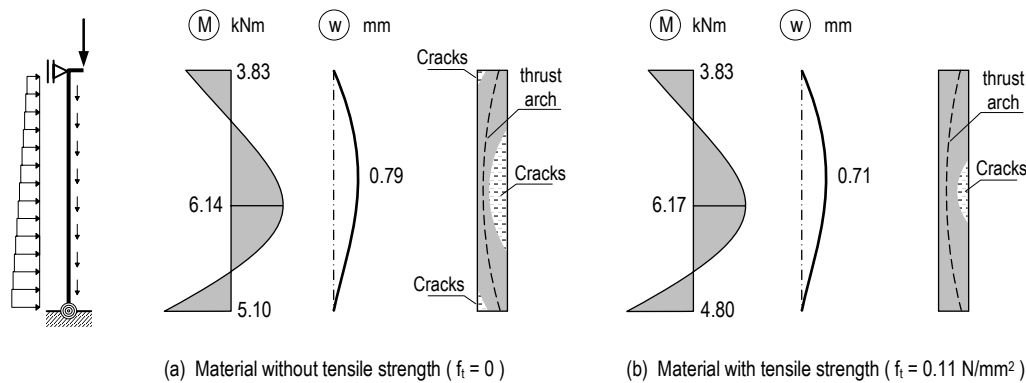


Figure 4. Internal forces, displacements and cracked regions for a) material without tensile strength and b) with limited tensile strength (perfectly brittle material behaviour)

After placing the backfill the wall is bent inward. The total displacement (difference to initial state without earth pressure) now evaluates to 0.79 mm when presuming no-tension material. With limited tensile strength (see Figure 4b) this value is slightly smaller; however the cracked zones reduce significantly.

It can be observed that displacement necessary to allow for active earth pressure conditions is not reached (greater than approx. 2.5 mm, see first part of this paper). Furthermore part of this deflection is already present before the compaction of the backfill material. The reduction of

earth pressure associated with the transition in active earth pressure conditions however can only take place if the deflection can and does further increase after the compaction. An increased earth pressure would lead to a further crack propagation which eventually reduces the bending stiffness of the wall and thus results in larger displacements. This self-calibrating process can only be effective if there is no further compaction of the soil thereafter and the wall itself possesses sufficient ductility. This behaviour has been captured by the model, where the vertical load could be reduced to 28.1 kN/m (with progressively increasing deflections).

Vogt came to comparable findings as the result of his research work on interaction between wall movement and earth pressure (Vogt 1984).

Three-dimensional Finite Element Models

As already mentioned, the consideration of a possibly biaxial load transfer mechanism allows a reduction of the required design load (inferior value) or a reduced wall thickness. In order to realistically model the biaxial load transfer mechanism a detailed three-dimensional finite element model was considered. An explicit modelling of the concrete slab at the top (using reduced elastic properties to simulate a partially cracked state) further improves the quality of the results as in this way the development of the eccentricity at the top of the wall is captured correctly. The applied modelling strategy is based on the assumption that the nonlinear behaviour of the basement wall is governed by the interface failure due to bending action, which complies with experimental evidence for large unit sizes and low vertical loads. Thus the interface behaviour was defined using the *Coulomb* friction law, neglecting any tensile strength perpendicular to the bed joints.

The material properties used in the numerical analyses were chosen on the basis of the German design code DIN 1053-100 (see Table 2).

Table 2. Material properties used in finite element analyses

	Masonry	Concrete
Modulus of elasticity (MN/m ²)	10 000	20 000 (30 000 for concrete frame)
Poisson ratio	0.2	0.2
Coefficient of friction	0.6	—
initial shear strength (MN/m ²) (bed joints and contact to concrete frame only)	0.36	—
effective tensile strength (MN/m ²) (concrete frame only)	—	2.2

In the models of the confined masonry wall the material of the concrete frame was given a tensile strength of 2.2 MN/m². In addition, reinforcement consisting of 4 steel bars with a modulus of elasticity of 200 000 MN/m² was introduced using discrete truss elements in each member of the concrete frame.

A simplified loading scenario was considered in order to alleviate the effort required for interpretation of the results. The simplifications consist of assuming a linearly increasing earth pressure (increasing with overburden depth), where the ground surface coincides with the top of the wall, and of neglecting live load on the soil. Thus the load bearing capacity of the wall under consideration can be expressed in terms of the maximum allowable earth pressure at the bottom of the wall, and can be readily compared to the results from models with varied parameters. During the simulation the earth pressure was incrementally increased starting from zero until the global stiffness matrix became singular, that is no static state of equilibrium could be found any more. The results obtained using the procedure represent conservative approximations of the exact load-bearing capacities since numerical instabilities usually provoke a (slightly) premature termination of the simulation process.

Common Wall Structures

A summary of the results obtained, extended by a comparison with the results from the analytical model presented in the first part of this paper is shown in Table 3. This was based on the inverse relationship given in eq. (4), adjusted to meet the simplified loading scenario introduced above and a limitation of the eccentricity of the normal force to $0.45t$. It should be noted that the analytical solution strongly depends on the procedure chosen to calculate the reaction forces of the concrete slab supported by the basement wall.

Table 3. Summary of bearing strength obtained from finite element models and analytical solution (in terms of max. bearable earth pressure at base of the wall)

Free wall length (m)	3.50	2.00
$q_{\text{analytic}} (e_{\text{lim}} = 0.45 \cdot t) \text{ (kN/m}^2\text{)}$	10.2 – 12.3	13.9 – 18.3
$q_{\text{FEM}} \text{ (kN/m}^2\text{)}$	14.9	21.0 (16.6)*
$q_{\text{FEM}}/q_{\text{analytic}} (e_{\text{lim}} = 0.45 \cdot t)$	1.21 – 1.46	1.15 – 1.51

* The value in brackets stems from a model with a reduced overlapping length by 50%

It can be seen that the analytical model underestimates the load bearing capacity (in comparison to the three dimensional finite element analysis), even for the case of using highest vertical load at the top of the wall, which exists only in the middle region of the basement wall.

Regarding the displacement shape at the loading state of imminent failure there is a great similarity between all investigated models. At the inner surface of the wall the bed joints open up mainly at mid-height. Additional joint openings are seen to develop diagonally (stepwise) towards the corners of the wall (Figure 5) – resembling the usual pattern known from the classical yield-line theory. Although these joint-openings seem to dominate the picture, the gap widths are only 0.02 to 0.1 mm. At the outer surface of the wall the only gaping joints appear right above the foundation and just underneath the concrete slab. The effect responsible for the differences in capacities between the analytical und the 3D finite element models can be identified as additional load redistribution along the wall length. With increasing earth pressures the rotation of the wall top in the middle region of the wall (see Figure 5) exerts an uplifting action onto the concrete slab, which leads to a partial shift of the

reaction forces from the ends into the middle region of the wall. Evidently, this effect is inversely proportional to the length of the basement wall.

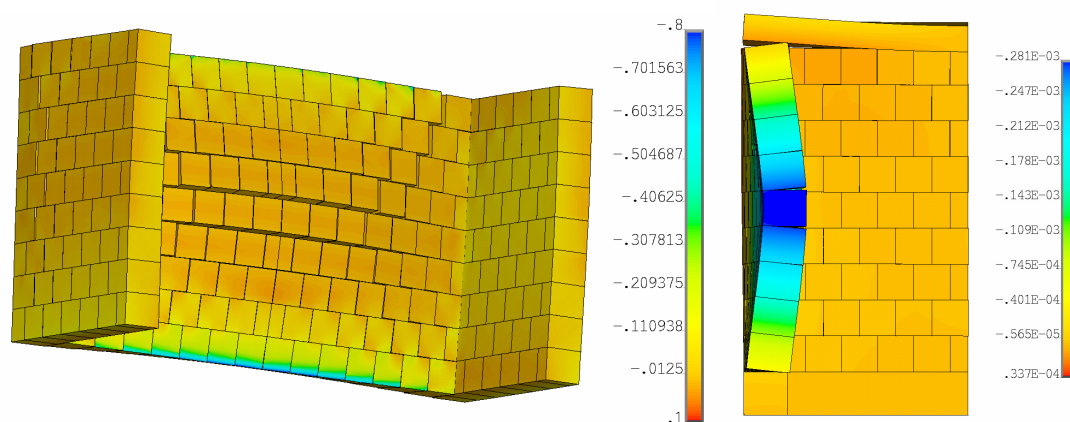


Figure 5. Basement wall $l = 3,50$ m – view from inside the basement (displacements 700 times magnified, contours for vertical stresses in (MN/m²)) and vertical section through wall (displacements in (mm) 1000 times magnified)

Confined Masonry

Compared to common masonry basement walls the load bearing capacity of confined masonry is substantially higher (for low vertical loads at top of wall). The increase of capacity depends significantly on the spacing of the vertical concrete columns. This not only allows for a biaxial load transfer but also effectively constrains the uplifting of the concrete slab due to the rotation of the wall top. This again results in an increased compressive force at the top of the wall and thus in a higher bending strength. For example, in the finite element model with a wall length of 3.5 m, the compressive force in mid-height was increased by this effect from 13.8 kN/m at the beginning to 37.4 kN/m at the point of immanent failure, and the bearing capacity was increased by a factor of 2.5 compared to unconfined masonry.

The values of the highest sustainable earth pressure were derived from models with a rigid connection of the horizontal beam at the top and the adjacent concrete slab. If this connection is removed, the sustainable earth pressure dramatically reduces to only 11.8 kN/m² for the 3.5 m long wall (approximately equal to the performance of the unconfined wall). The reason for this behaviour is the nearly unconstrained torsion of the upper beam, which prevents the increase of the vertical force. The effect of the reduced vertical force is clearly visible in Figure 6, where the maximum eccentricity (which coincides with the maximal crack depths) occurs further up the wall height.

It may be interesting to note, that a similar increase in load bearing capacity can also be achieved in the absence of any initial shear strength (48.1 kN/m² for 3.5 m long wall). Here self weight and a coefficient of friction of 0.6 are sufficient to restrain an initial deflection of the wall and thus the load transfer by arching effects in vertical direction. However, the load transfer remains mainly uniaxial because of the slip in the interface between the units and the vertical concrete members.

The crack pattern in the reinforced concrete frame is asymmetric, caused by the equally asymmetric loading and deflection due to the asymmetric overlapping pattern (Figure 7). This

also leads to a one-sided contact failure between the masonry and the concrete frame. The load transfer thus becomes effectively uniaxial.

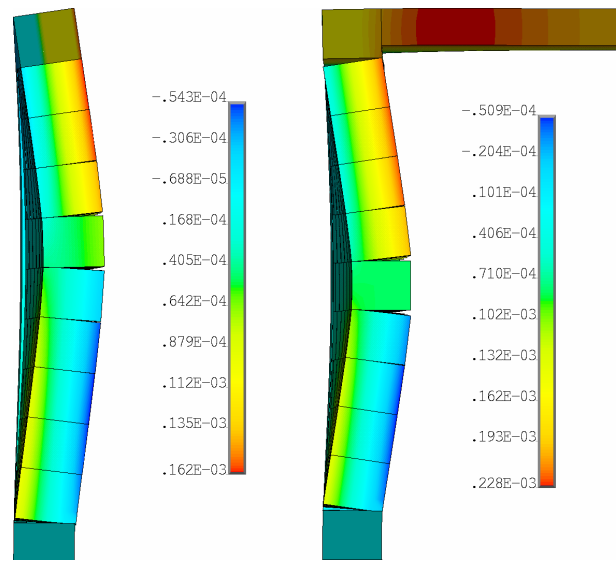


Figure 6. Confined masonry basement wall $l = 3.50$ m – vertical displacements in (mm): left without, right with restraint torsion of reinforced concrete beam (deformation are 500 times magnified)

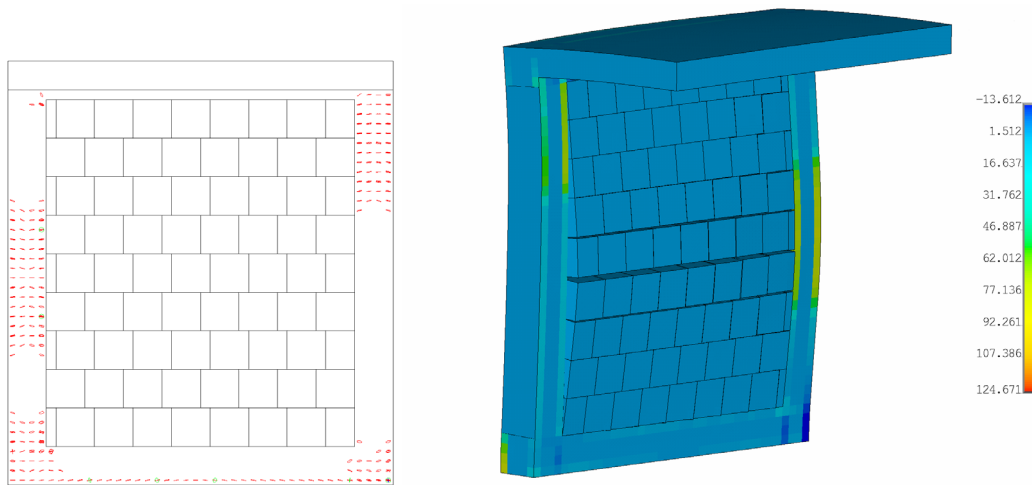


Figure 7. Confined masonry basement wall $l = 2.00$ m – cracks and reinforcement stresses in (MN/m^2) for overlapping of one quarter unit length

CONCLUSION

The aim of this paper is to analyse the subject of the behaviour of masonry basement walls, especially the critical case when the vertical loads are very low. The basic assumptions included in the design code requirements (DIN 1053 and EC 6-3) have been demonstrated and the performance of the design formulae has been compared with more detailed, numerical solutions. The definite conclusions can be drawn, that design checks based on the formulae given by the German and European Codes are over-conservative and thus unutilised capacity reserves do exist. The three-dimensional numerical analysis of masonry basement walls

demonstrates the load transfer mechanisms involved in the real behaviour. It becomes evident, that displacement constraints and compliance deformations, which are commonly neglected in practical design checks, substantially increase the bearing strength of the basement walls. These effects are non-linear by nature, combining geometric and physical nonlinearity.

REFERENCES

Ackermann, W., Knobloch, C.: „Gemauerte erddruckbelastete Kelleraußenwände sind nicht mehr standsicher“, *Der Sachverständige* Vol. 33 (2006) No. 11, pp. 335-341.

Broms, B.: „Berechnung des Erddruckes auf Kellerwände“. *Mauerwerk* Vol. 11 (2007) No. 3, pp. 129-134.

DIN 1053-100:2007-09: „*Mauerwerk*. Berechnung auf der Grundlage des semiprobabilistischen Sicherheitskonzepts“. DIN, Beuth Verlag: Berlin 2006.

EN 1996-3: 2006-01: “*Eurocode 6 - Design of masonry structures. Simplified calculation methods for unreinforced masonry structures*”. CEN: Brussels 2006.

Mann, W., Bernhardt, G.: „Rechnerischer Nachweis von ein- und zweiachsig gespannten gemauerten Wänden, insbesondere von Kellerwänden auf Erddruck.“ In: *Mauerwerk-Kalender* 19 (1984). Ed. P. Funk. Ernst & Sohn: Berlin, pp. 69-84.

Mann, W., “The Load-bearing behaviour of bi-axially spanned masonry walls subjected simultaneously to horizontal and vertical loading.” *Proceedings of 7th IBMaC*, Melbourne, Australia, 1985, pp. 1195 - 1204.

Spotka, H.: „Einfluss der Bodenverdichtung mittels Oberflächen-Rüttler auf den Erddruck einer Stützwand bei Sand“. Diss., Mitt. No. 9 Inst. für Grundbau und Bodenmechanik Universität Stuttgart 1977.

Tengvall, I.: ”Grundmurskonstruktion för smahus med källare”. *Väg- och vattenbyggaen*, 1968, No 1-2, pp. 9-12.

Vassilev, T. et al.: “Numerical Simulation of Masonry under Combined Lateral Loading and Compression.” In: *Proceedings of the 13th IBMaC* Amsterdam, 2004, pp. 391-400.

Vassilev, T.; Jäger, W.: „Numerische Simulation des Knickverhaltens von Mauerwerk.“ *Bautechnik* Vol. 81 (2004) No. 6, pp. 461-467.

Vassilev, T.: „Verformungsverhalten von Kellerwänden unter Berücksichtigung des tatsächlichen Materialverhaltens.“ *Mauerwerk* Vol. 11 (2007) No. 3, pp. 143 - 149.

Vogt, N.: „*Erdwiderstandsermittlung bei monotonen und wiederholten Wandbewegungen in Sand*“. Diss., Mitt. No. 22 Inst. für Grundbau und Bodenmechanik Universität Stuttgart, 1984.